A metabolomic comparison of urinary changes in type 2 diabetes in mouse, rat, and human

R. M. Salek, M. L. Maguire, E. Bentley, D. V. Rubtsov, T. Hough, M. Cheeseman, D. Nunez, B. C. Sweatman, J. N. Haselden, R. D. Cox, S. C. Connor and J. L. Griffin

Physiol. Genomics 29:99-108, 2007. First published 26 December 2006;
doi: 10.1152/physiolgenomics.00194.2006

Physiol Genomics 29: 99–108, 2007.
First published December 26, 2006; doi:10.1152/physiolgenomics.00194.2006.

A metabolomic comparison of urinary changes in type 2 diabetes in mouse, rat, and human

R. M. Salek,[1]* M. L. Maguire,[1]* E. Bentley,[2] D. V. Rubtsov,[1] T. Hough,[3] M. Cheeseman,[3] D. Nunez,[4] B. C. Sweatman,[4] J. N. Haselden,[4] R. D. Cox,[2] S. C. Connor,[4] and J. L. Griffin[1]

[1]*Department of Biochemistry, University of Cambridge, Cambridge;* [2]*Mammalian Genetics Unit, Medical Research Council (MRC) Harwell, Oxfordshire;* [3]*The Mary Lyon Centre, MRC Harwell, Harwell, Oxfordshire; and* [4]*Safety Assessment, GlaxoSmithKline, Ware, Herts, United Kingdom*

Submitted 5 September 2006; accepted in final form 15 December 2006

Salek RM, Maguire ML, Bentley E, Rubtsov DV, Hough T, Cheeseman M, Nunez D, Sweatman BC, Haselden JN, Cox RD, Connor SC, Griffin JL. A metabolomic comparison of urinary changes in type 2 diabetes in mouse, rat, and human. *Physiol Genomics* 29: 99–108, 2007. First published December 26, 2006; doi:10.1152/physiolgenomics.00194.2006.—Type 2 diabetes mellitus is the result of a combination of impaired insulin secretion with reduced insulin sensitivity of target tissues. There are an estimated 150 million affected individuals worldwide, of whom a large proportion remains undiagnosed because of a lack of specific symptoms early in this disorder and inadequate diagnostics. In this study, NMR-based metabolomic analysis in conjunction with multivariate statistics was applied to examine the urinary metabolic changes in two rodent models of type 2 diabetes mellitus as well as unmedicated human sufferers. The *db/db* mouse and obese Zucker (*fa/fa*) rat have autosomal recessive defects in the leptin receptor gene, causing type 2 diabetes. ^{1}H-NMR spectra of urine were used in conjunction with uni- and multivariate statistics to identify disease-related metabolic changes in these two animal models and human sufferers. This study demonstrates metabolic similarities between the three species examined, including metabolic responses associated with general systemic stress, changes in the TCA cycle, and perturbations in nucleotide metabolism and in methylamine metabolism. All three species demonstrated profound changes in nucleotide metabolism, including that of *N*-methylnicotinamide and *N*-methyl-2-pyridone-5-carboxamide, which may provide unique biomarkers for following type 2 diabetes mellitus progression.

metabonomics; metabolic syndrome; biofluids; Zucker rat; *db/db* mouse; nuclear magnetic resonance spectroscopy; leptin resistance

TYPE 2 DIABETES MELLITUS (T2DM) is among the most prevalent diseases in the world. There are an estimated 150 million affected individuals worldwide of whom a large proportion remains undiagnosed because of a lack of specific symptoms early in this disorder and inadequate diagnostics (26). It is associated with microvascular (neuropathy, nephropathy, and retinopathy) and macrovascular (atherosclerotic-related vascular disease, coronary heart disease, cerebrovascular disease, and peripheral vascular disease) complications (46).

To improve the understanding of the early stages of T2DM development, a number of animal models have been developed. We have considered two such models: the C57BL/KsJ *db/db* mouse and the obese Zucker (*fa/fa*) rat. The *db/db* mouse has a single-gene autosomal recessive defect in the leptin receptor gene. Leptin is a hormone produced primarily by white fat cells and is involved in regulating body weight and energy homoeostasis (31). In the *db/db* mouse, the concentration of insulin steadily increases with age until ~8–10 wk, after which the concentration declines to below control nondiabetic levels (35). The *db/db* mouse produces clinical signs of leptin resistance, hyperphagia, obesity, and subsequent insulin resistance. The relevance of this model to human T2DM has been debated, as mutations in this gene in humans are rare (40), but the subsequent T2DM is characteristic of the metabolic changes in humans with severe disease. The obese Zucker (*fa/fa*) rat (9, 47) also has a single-gene autosomal recessive mutation in the leptin receptor (43), causing clinical signs of leptin resistance, obesity, hyperlipidemia, hyperinsulinemia, and, post-6 wk of age, fasting hyperglycemia and T2DM (32). The heterozygous (*fa/+*) lean genotype rats remain normoglycemic. Because the relevance of the *db/db* mouse and Zucker rat models of T2DM has been questioned, this study aims to determine any metabolic similarities or differences among the two rodent models and human subjects with T2DM, and in particular to identify any important perturbations in metabolism common to all three species.

Here we describe the application of ^{1}H-NMR spectroscopy-based metabolomics, combined with multivariate and univariate statistics, to investigate the urinary metabolic profiles in two animal models of T2DM. We have compared these metabolic changes with perturbations observed in a human population of unmedicated diabetic patients who have good daily dietary control over their blood glucose concentrations by following the guidelines on diet issued by the American Diabetes Association. Diabetes can lead to pathological concentrations of several metabolites in plasma that are ultimately detected in urine (27, 33), an effect exacerbated by glycosuria. High blood glucose concentrations cause impaired solute reabsorption from the tubular lumen and reduced efficiency of the epithelium (7, 27). Multivariate analysis has been applied to delineate the effects of hyperglycemia and general metabolic stress responses from other potentially more discriminatory metabolic pathways.

MATERIALS AND METHODS

db/db mouse urine collection. All animal procedures were approved and conformed to the United Kingdom Home Office guidelines concerning laboratory animal care and welfare (Scientific Procedures Act 1986). C57BL/KsJ *db/db* mice and their controls were maintained in a specific pathogen-free (SPF) colony at MRC Harwell, UK. Mice were reared in individually ventilated racks (Techniplast) in

* R. M. Salek and M. L. Maguire contributed equally to this work.

Article published online before print. See web site for date of publication (http://physiolgenomics.physiology.org).

Address for reprint requests and other correspondence: J. L. Griffin, Dept. of Biochemistry, Univ. of Cambridge, Bldg. O, Downing Site, Tennis Court Road, Cambridge, CB2 1QW, UK (e-mail: jlg40@mole.bio.cam.ac.uk).

a 12:12-h light-dark cycle at 20–22°C and 50–60% relative humidity on grade 6 sawdust bedding (Datesand). Mice were fed standard laboratory chow (Rat and Mouse No. 3 Breeding, Special Diets Services) ad libitum (25). Urine samples were collected from animals in individual urine collection cages after acclimatization for 24 h onto sodium azide and stored at −80°C before analysis. Urine samples (142) were collected from wildtype and *db/db* homozygote and heterozygote male and female mice aged 8–24 wk (Supplemental Table 1; supplemental data are available at the online version of this article). Body mass, plasma glucose, and plasma insulin concentrations were also measured (Supplemental Table 2). All *db/db* mice exhibited a marked diabetic phenotype as confirmed by blood biochemistry analysis (data not shown).

Zucker rat urine collection. Obese Zucker (*fa/fa*) rats and lean (*fa/+*) rats were maintained in stable colonies at GlaxoSmithKline (Ware, UK; temperature 21 ± 2°C, relative humidity 55 ± 10%, and fluorescent lighting 06.00–18.00 GMT). Rats were fed on standard laboratory chow (2014 Teklad Global 14% Protein Rodent Maintenance Diet, Harlan) ad libitum. Urine samples were collected from male rats ($n = 8$ for lean and fatty Zucker rats) housed in individual urine collection cages after acclimatization and collected over solid CO_2 at two intervals (0–8 and 8–24 h) at 1, 4, 8, and 12 wk. Urine samples (128) were collected and stored at −80°C. Body mass and food and water consumption were monitored daily. All *fa/fa* rats exhibited a marked diabetic phenotype confirmed by blood biochemistry analysis (data not shown).

Human urine collection. For the clinical study, participants gave informed consent that met all criteria required for entry into the study (see supplementary information for details). The study was conducted in accordance with "good clinical practice" and all applicable regulatory requirements, including the 1996 version of the Declaration of Helsinki. GlaxoSmithKline provided the investigators with any relevant document(s)/data that were needed for IEC/IRB review and approval of the study. For the human studies, midstream urine (~15 ml) samples were collected and frozen from each volunteer. In total, 84 samples were collected from 12 healthy volunteers (7 time points, 8 males and 4 females) and 50 samples from 30 T2DM patients (1–3 time points, 17 males and 13 females) with well-controlled blood glucose maintained at normal concentrations by diet, following the guidelines issued by the American Diabetes Association, rather than medication. The healthy subjects were aged 18–55 yr, had a body mass index (BMI) ≥19 and ≤30 kg/m^2 and a body mass ≥50 kg and ≤113 kg, and were free from any major disease or pregnancy. The T2DM patients were aged 30–65 yr (mean 56 ± 9 yr), had a BMI >25 and <40 kg/m^2, weighed between 65 and 140 kg (mean 95 ± 19 kg), and were taking at most one oral anti-diabetic drug. T2DM patients agreed to stop treatment with oral anti-diabetic agents during the study. Subjects went through a washout period of 4 wk before sample collection and abstained from alcohol during the study; diet was controlled throughout the study. Clinical biochemical measurements for the T2DM patients during the study were taken, with most analytes within normal range; cholesterol, glycosylated hemoglobin, high-density lipoprotein (HDL), and triglycerides were slightly elevated (Supplemental Table 3). Stringent selection criteria were also placed on blood pressure and renal function to exclude diabetic patients with complications associated with extreme obesity, high blood pressure, and renal dysfunction (Supplemental Materials). Two outlying diabetic patients were identified as a result of over-the-counter medicine (paracetamol) in the samples. These data were excluded from further analysis.

NMR acquisition and processing methods. When placed in a strong magnetic field, each chemically distinct proton in a solution will exhibit a unique chemical shift that depends on the exact stereochemical environment surrounding that proton. The intensity of this signal depends on the concentration of the proton, and hence of the metabolite, in the solution. By assigning each chemical shift to a metabolite and analyzing the relative changes in signal intensity between the disease and control samples, we could monitor the changes in metabolite concentration for a wide range of metabolites simultaneously.

Aliquots of either 200-μl (mice) or 400-μl (rat and human) urine samples were made up to 600 μl with phosphate buffer (0.2 M, pH 7.4) and any precipitate removed by centrifugation. In total, 500 μl of supernatant were transferred to 5-mm NMR tubes with 100 μl of sodium 3-trimethylsilyl-(2,2,3,3-$^2H_4$)-1-propionate (TSP)/D_2O/sodium azide solution (0.05% wt/vol TSP in D_2O and 1% wt/vol sodium azide).

NMR spectra of the *db/db* mice urine samples were recorded on a Varian INOVA spectrometer (Varian, Palo Alto, CA) at a proton frequency of 400.1 MHz, rat urine spectra on a Bruker DRX600 spectrometer (Bruker BioSpin, Rheinstetten, Germany) at a proton frequency of 600.1 MHz, and human urine spectra on a Bruker DRX700 NMR spectrometer at a proton frequency of 700.1 MHz (see Supplemental Materials). The one-dimensional (1D) NOESY pulse sequence with water presaturation was used throughout. NMR spectra were assigned with reference to the literature (15, 30) or confirmed by 2D spectroscopy including homonuclear ^{1}H-^{1}H correlation spectroscopy (COSY), ^{1}H-^{13}C heteronuclear signal quantum correlation (HSQC), and ^{1}H-^{13}C heteronuclear multiple bond correlation (HMBC) spectroscopy.

Spectra were processed using ACD/1D NMR Manager 8.0 with Intelligent Bucketing Integration (Advanced Chemistry Development, Toronto, ON, Canada). Spectra were integrated 0.20–9.30 ppm excluding water (4.24–5.04 ppm), glucose (3.19–3.99 ppm, 5.21–5.27 ppm), and urea (5.04–6.00 ppm). Intelligent bucketing ensures that bucket edges do not coincide with peak maxima, preventing resonances from being split across separate integral regions; a 0.04-ppm bucket width and a 50% looseness factor were used. All spectra were normalized to total area excluding the water, urea, and glucose regions.

Confirmation of nucleotide identification. Because of the relatively low concentration of nucleotides precluding definitive assignment by 2D spectra, LC-MS was used to confirm their presence. Urine samples were analyzed for *N*-methyl-2-pyridone-5-carboxamide (2PY) and *N*-methyl-4-pyridone-5-carboxamide (4PY) using an API-3000 HPLC/MS/MS (Applied Biosystems/MDS SCIEX, Foster City, CA) with Agilent 1100 binary solvent delivery system HPLC and 100 × 2.1 mm inner diameter, 4-m Synergi Polar column (Phenomenex, Torrance, CA). The lower limit of detection for all analytes was 1.0 μg/ml. Data were acquired and quantified using Analyst Version 1.4 (Applied Biosystems/MDS SCIEX, Foster City, CA) and SMS2000 Version 1.4 (GlaxoSmithKline, in-house).

Chemometric analysis of the data. Multivariate data analysis was carried out using SIMCA-P+ 10.0 (Umetrics, Umea, Sweden). Data were mean centered and Pareto scaled (weighted by $1/\sqrt{\sigma}$ of the mean-centered variable) before analysis. Pareto scaling is a compromise between mean centering, which may fail to pick out small changes in metabolite concentrations, and scaling to unit variance, which gives equal weight to baseline imperfections, noise, and defined signals in the NMR spectrum.

Principal components analysis (PCA) was used to examine inherent clustering and correlations within the data. A principal component (PC) is a weighted linear combination of each of the original NMR variables so that the original data matrix is compressed into a smaller number of "latent variables," typically three to four PCs for NMR data. The weight given to each variable within a PC describes how influential that variable is in relation to the other variables. The information that is not captured in the first PC forms the residuals through which the second PC is calculated; all PCs are mutually orthogonal.

Partial least squares (PLS) techniques were used to assess correlation between the observed NMR data and other factors such as age. A PLS model is expressed as a set of *X*-scores (NMR spectral regions) and *Y*-score vectors (e.g., age) with corresponding *X*- and *Y*-weight vectors for a set of PLS model dimensions. Each dimension expresses a linear relation between an *X*-score and *Y*-score vector with the weight vectors describing how the *X*- and *Y*-variables are combined to

give the *X*- and *Y*-score vectors. The model corresponds to fitting the lower-dimensional line, plane, or hyperplane simultaneously to the *X*- and *Y*-data as points in multidimensional space that best approximate the original data. The PLS model can be used to estimate the *Y*-variables corresponding to a given set of *X*-variables, (e.g., estimate the age of an organism given an NMR spectrum). In PLS-discriminant analysis (PLS-DA), dummy variables representing the class (e.g., disease) of each sample form the *Y*-matrix. PLS-DA was used for classification of samples where the PCA models were dominated by effects such as species or gender differences.

To assess which metabolite regions were responsible for a given classification, a twofold procedure was used combining both multivariate data analysis (MVDA) and univariate data analysis (UVDA) approaches. For each PLS-DA component responsible for class separation, cross-validation jack-knifing was used to calculate the magnitude and standard error for each variable coefficient, and Student's *t*-test was used to determine which coefficients differed significantly from zero. For the MVDA component of the combined analysis, a coefficient scored 0.15 if it had $P < 0.20$, 0.50 if $P < 0.10$, and 1.00 if $P < 0.05$.

Univariate statistical tests were carried out on bucketed NMR spectra. Each bucket was treated as an independent variable with two statistical samples: control and disease. Evidence for a statistically significant difference between the distributions of the two samples was based on the parametric Student's *t*-test (assumes normal distribution) and *F*-test (comparison of variances), and the nonparametric Kruskal-Wallis (generalized analysis of variance with no assumption of distribution form) and Kolmogorov-Smirnov tests (comparison of distribution shape). A threshold *P* value of 0.05 was used for each test. In the combined analysis, for each test passed the variable scored 0.25, giving a maximum score of 1.00. For the combined MVDA/UVDA analysis, metabolite regions scoring above 1.0 out of a maximum of 2.0 were considered significant.

For all models, disease/control classification was verified using a Cooman's plot (13), and the model was validated by random permutation of the *Y*-matrix (see Supplemental Materials) (14).

RESULTS

Analysis of db/db mice. The metabolic profiles of urine samples from *db/db* and wildtype mice indicated high glucose concentrations in the *db/db* samples (Fig. 1*A*). Because an increased urinary glucose concentration is well documented in diabetes, the glucose resonances were excluded

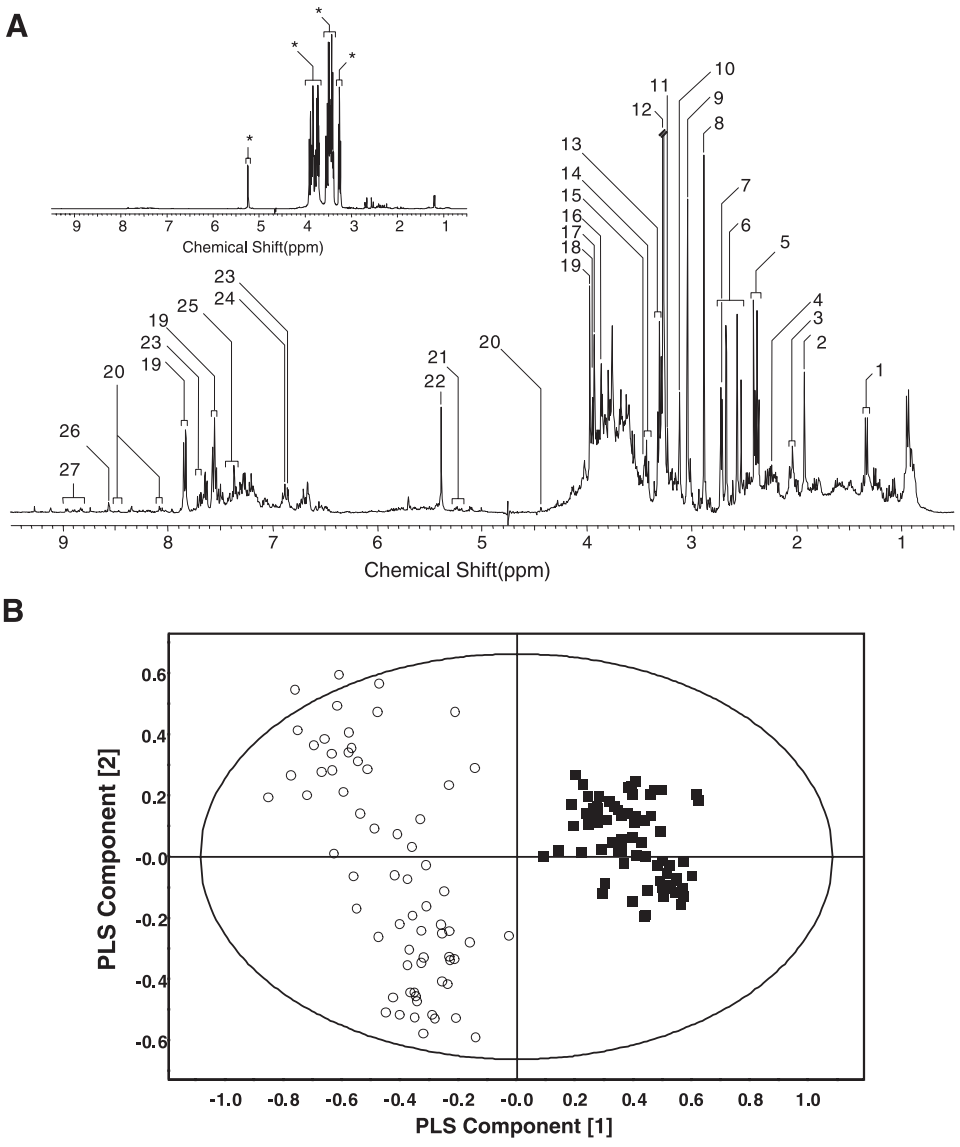

Fig. 1. Analysis of *db/db* mouse urine. *A*: 400-MHz ^{1}H-NMR spectrum of mouse urine. Main plot shows an NMR spectrum of a mouse heterozygous for the *db* knockout with assignments. *Inset*: spectrum recorded for a urine sample from a mouse homozygous for the *db* knockout; the multiplets corresponding to the glucose resonances are indicated with asterisks (*). These regions were excluded from the statistical analyses. *1*, lactate; *2*, acetate; *3*, *N*-acetyl groups; *4*, acetone; *5*, β-hydroxybutyrate/unknown multiplet; *6*, citrate; *7*, DMA; *8*, TMA; *9*, creatine; *10*, malonate; *11*, choline; *12*, TMAO; *13*, tryptophan; *14*, taurine; *15*, acetoacetate; *16*, guanidoacetate; *17*, glycolate; *18*, creatine; *19*, hippurate; *20*, NMN acid; *21*, α-glucose; *22*, allantoin; *23*, 4-aminohippurate; *24*, 3,4-dihydroxymandelate; *25*, PAG; *26*, 4PY; *27*, NMN amide; *, glucose. *B*: PLS-DA score plot for the *db/db* mouse, separating the diseased (■, homozygote) mouse from the control (○, heterozygote and wildtype). PLS, partial least squares; DMA, dimethylamine; TMA, trimethylamine; TMAO, trimethylamine-*N*-oxide; NMN acid, *N*-methylnicotinate; PAG, phenyl acetylglycine; 4PY, *N*-methyl-4-pyridone-5-carboxamide; NMN amide, *N*-methylnicotinamide; PLS-DA, PLS-discriminant analysis.

from the subsequent analyses described for mouse, rat, and human data. PCA models of the NMR data of *db/db* mice (not shown) highlighted three samples with abnormally high β-hydroxybutyrate concentrations (doublet at 1.20 ppm, multiplet at 2.37 ppm). Increased β-hydroxybutyrate reflects the onset of ketosis and is a marker of decreased pancreatic β-cell insulin production observed in older *db/db* mice (11, 37). While it was important to characterize the metabolic profile associated with this alteration, the biochemical status of these animals was very different from the rest of the group; these individuals were excluded from further investigation. *db/+* mice co-clustered with wildtype mice, using PCA or PLS-DA, indicating that the heterozygous mice were metabolically indistinguishable from their wildtype siblings (data not shown); heterozygous and wildtype mice were therefore treated as a single group in further analyses. The *db/db* mice formed a cluster distinct from the combined wildtype/heterozygous group in both PCA (data not shown) and PLS-DA models ($Q^2 = 0.93$, $R^2 = 0.95$, 4 components) (Fig. 1*B* and Supplemental Materials). The disease process was the dominant effect (PC1), with the wildtype/heterozygous group also separated according to gender (PC2); this sex difference was not as apparent in the disease group. This overlap of male and female groups was due in part to the presence of protein in the urine as determined by visual inspection of the NMR spectra.

Analysis of the coefficients of the PLS-DA model identified metabolites that correlated with the disease process. These changes included decreases in *N*-acetyl groups (including glycoproteins), methionine, 2-oxoglutarate, creatine, and malonate and increases in glycerol, citrate, dimethylamine (DMA), trimethylamine (TMA), glutamate/glutamine, succinate, β-hydroxybutyrate, and lactate (Supplemental Table 4). One complicating factor with these data was the broad baseline resonances in the NMR spectra of male mouse urine arising from proteinuria. Although these resonances were more intense in the *db/db* spectra, they were present in all spectra. The aliphatic (0.2–1.4 ppm) and aromatic regions (7.0–8.2 ppm) were most affected, but it was not possible to directly quantify the total amount of urinary protein because of the broad resonances involved.

Similar metabolites were shown to be important for disease/control discrimination for both males and females when each gender was modeled separately (data not shown). This finding confirms earlier conclusions from the PCA and PLS-DA of the full data set where disease/control separation was the dominant source of variation (PC1) with gender separation orthogonal (PC2). This absence of disease/gender correlation was confirmed by the lack of any disease/gender interaction observed in the Kruskal-Wallis test results.

PLS models were built to describe the age trend for the wildtype/heterozygous samples and for the *db/db* samples for both male and female samples together (Supplemental Fig. 1, *D* and *E*) and separately (not shown). For each PLS model, the mouse data for either *db/db* or the wildtype/heterozygous group from all age groups combined were used to build the models. To examine whether these age trends were the same for the wildtype/heterozygous and homozygous groups, each model was used to predict the ages of the group not used to build the PLS model. The models built using the wildtype/heterozygous data sets were able to predict the ages of the wildtype/heterozygous samples but were unable to predict the ages of the *db/db* mice (data not shown) and vice versa. This indicated that the change in urinary metabolite profile with age is different for the *db/db* mice and wildtype/heterozygous mice. The urinary excretion of β-hydroxybutyrate and acetone increased with age in *db/db* mice, whereas the TCA cycle intermediates citrate, 2-oxoglutarate, and fumarate as well as allantoin, creatine, *N*-methylnicotinamide (NMN amide), hippurate, meta-hydroxyphenyl-propionic acid (mHPPA), and indoxyl sulfate decreased with age.

Analysis of the Zucker rat data set. The urinary profiles of the Zucker fatty and lean rats were examined by MVDA and UVDA of ^{1}H-NMR spectra excluding the glucose resonances (Fig. 2*A*). For male Zucker rats, PCA ($Q^2 = 0.60$, $R^2 = 0.7$, 4 components) and PLS-DA ($R^2 = 0.95$, $Q^2 = 0.94$, 2 components) models separated the lean (*fa/+*) and fatty (*fa/fa*) rats (Fig. 2*B* and Supplemental Fig. 2*C*). While the disease separation dominated PC1, PC2 characterized differences in day/night metabolism. The *fa/fa* rats were distinguished clearly from *fa/+* rats by increased concentrations of a range of metabolites including α-hydroxy-*n*-butyrate, lactate, fumarate, taurine, betaine, citrate, free fatty acids, DMA, *N,N*-dimethylglycine (DMG), *cis*-aconitate, valine, lysine, glutamine/glutamate, succinate/malate, and formate, while 2-oxoglutarate, phenylacetyl-glycine (PAG), hippurate, allantoin, unassigned *N*-acetyl groups (including glycoprotein), proline, ornithine, and creatinine were decreased (Supplemental Table 5).

PLS models for *fa/fa* and *fa/+* rats were produced from the urinary profiles for all age groups, identifying trends associated within each group (considering day and night together and separately; Supplemental Fig. 2, *D* and *E*). When these models were used to predict the age of the other group (e.g., predicting the age of *fa/fa* rats using the *fa/+* PLS model), the predictions were poor. For *fa/fa* rats, the aging trend was associated with increases in *N*-acetyl groups, *N*-acetyl aspartate (NAA), acetamide, and oxaloacetate, and decreases in 2-oxoglutarate, *cis*-aconitate, DMA, DMG, tryptophan, and acetate.

Human diabetes patients. PLS-DA models ($R^2 = 0.67$, $Q^2 = 0.51$, and 3 components; males and females excluding outliers; Fig. 3*B* and Supplemental Fig. 3*C*) of the NMR urine profile from T2DM patients compared with that of healthy subjects (Fig. 3*A*) showed a large number of metabolites contributed to the separation of the models. These metabolites included amino acids, tryptophan/tryptamine, 2-oxoisovalerate, alanine, ornithine, leucine, isoleucine, valine, and histidine. In addition, increases in relative concentration were observed for acetoacetate, acetate, *n*-butyrate, α-hydroxy-*n*-butyrate, DMA, DMG, NMN amide, and NAA, with decreases for creatinine, *N*-acetyl groups (including glycoproteins), *N*-methylnicotinate (NMN acid), aminohippurate, hippurate, PAG, allantoin, fumarate, and succinate. MVDA and UVDA showed that ~60 chemical shift regions were responsible for robust classification of diabetic patients (Supplemental Table 6).

DISCUSSION

For all three species, the Kyoto Encyclopedia of Genes and Genomes pathways for which metabolite perturbations were observed were plotted as a pie chart (Fig. 4*A*). Along with the expected glycosuria, changes in the excretion of TCA cycle intermediates, polyols, amines, and amino acids were detected. A

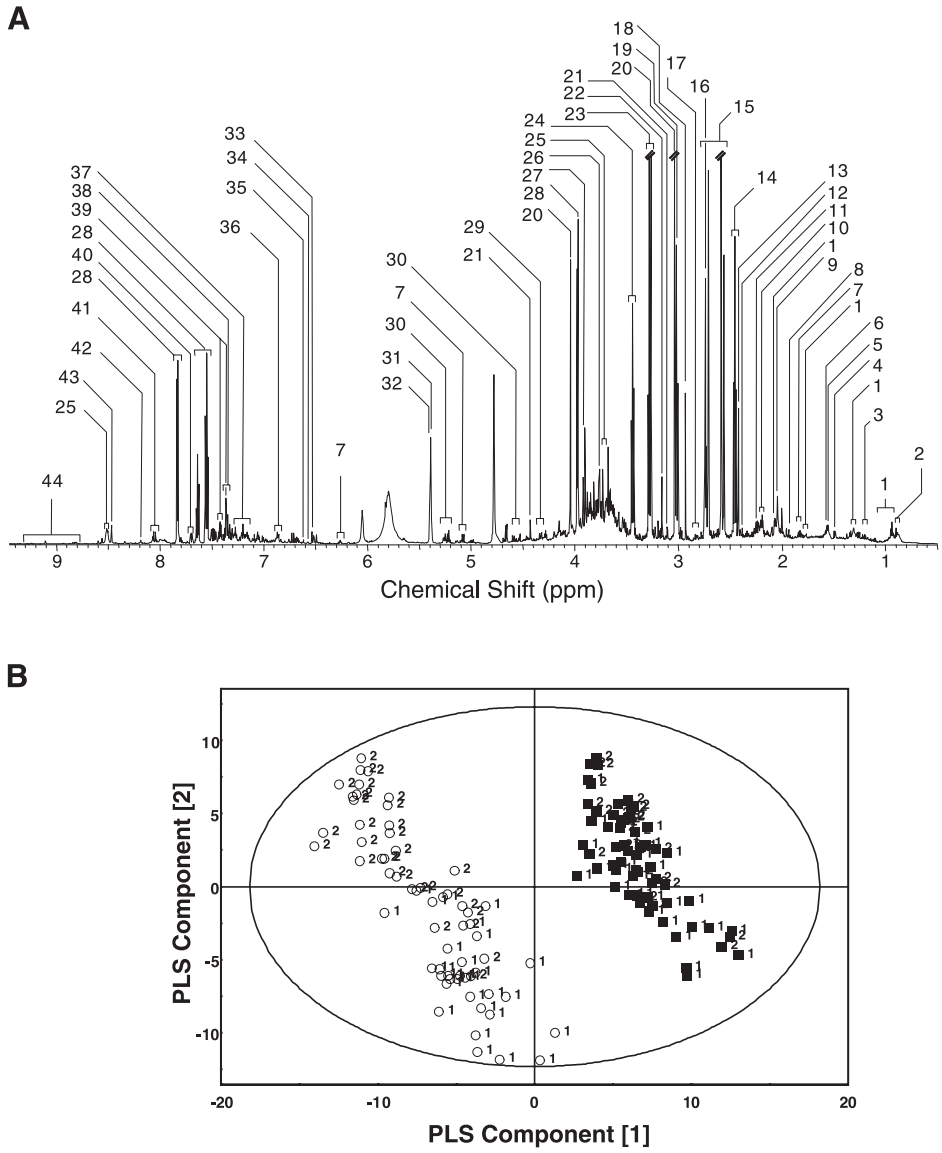

Fig. 2. Analysis of Zucker rat urine. *A*: plot shows a 600-MHz ^{1}H-NMR spectrum of *fa/+* Zucker rat with assignments. *1*, amino acids; *2*, α-hydroxy-*n*-butyrate; *3*, unknown doublet; *4*, alanine; *5*, adipate; *6*, *n*-butyrate; *7*, unknown triplet; *8*, acetate; *9*, *N*-acetyl aspartate (NAA); *10*, adipate; *11*, acetone; *12*, oxaloacetate; *13*, succinate; *14*, 2-oxoglutarate; *15*, citrate; *16*, DMA; *17*, 3-hydroxy propionic acid; *18*, *N,N*-dimethylglycine (DMG); *19*, 2-oxoglutarate; *20*, creatinine; *21*, unknown singlet; *22*, *cis*-aconitate; *23*, taurine + TMAO + betaine; *24*, taurine; *25*, unknown multiplet; *26*, DMG; *27*, betaine; *28*, hippurate; *29*, malate; *30*, galactose/glucose; *31*, allantoin; *32*, sucrose; *33*, fumarate; *34*, 4PY; *35*, *trans*-aconitate; *36*, 3-hydroxy propionic acid + 4-amino hippurate; *37*, tryptophan; *38*, phenylalanine; *39*, PAG; *40*, tryptamine; *41*, NMN acid; *42*, NMN amide; *43*, formate; *44*, NMN amide + NMN acid. *B*: PLS-DA score plot distinguishing Zucker lean *fa/+* (■) from *fa/fa* fatty rats (○) (R^2 = 0.95%, Q^2 = 0.94%, 2 components). ^{1}Samples collected during the day. ^{2}Samples collected during the night.

profound perturbation in nucleotide metabolism, previously linked with peroxisome proliferation, was also observed and may indicate a metabolic consequence of substrate excess in many tissues, especially the liver (36).

Methylamine metabolism and osmoregulation in T2DM. The increases in DMA, TMA, and DMG concentrations observed in humans, Zucker *fa/fa* rats, and *db/db* mice are indicative of a change in the balance of methylamine metabolism. Methylamines are important osmoregulatory compounds (17, 21) and are produced via degradation of dietary choline to TMA and its di- and monoamine metabolites by gut microflora (2). Polyamines are also produced systemically through breakdown of choline into betaine and DMG. Gavaghan et al. (18) observed that when the population of gut microflora is reduced, the urinary concentration of betaine is increased relative to that of trimethylamine-*N*-oxide (TMAO) and DMA (18). The major betaine resonances overlap with those from glucose and hence were excluded from the analysis. However, visual inspection of the spectra showed that betaine increased in diabetic humans and Zucker *fa/fa* rats consistent with a general perturbation in choline degradation. Altered choline degradation in all three species may be a reflection of altered demand, possibly by altered lipoprotein turnover/biosynthesis, alterations in gut microflora or as an osmotic compensation for raised blood glucose concentrations.

Kidney function in T2DM. The creatinine depletion observed in urine from the animal models and T2DM patients may have arisen because of a variety of reasons such as changes in muscle mass, creatinine reabsorption, cell leakage, and changes in caloric intake. However, a decline in the renal glomerular filtration rate (GFR) associated with diabetic nephropathy (8, 29, 39) would not only explain this observation but also a variety of other metabolite changes. For example, reduced urinary allantoin excretion is also indicative of reduced GFR as allantoin is not reabsorbed across the proximal tubule, and thus its urinary concentration is thought to accurately reflect glomerular filtration (5, 19). Reduced urinary creatinine has also been observed in older Zucker rats (>13 wk) exhibiting albuminuria and glomerulosclerosis (41) with altered renal tubular function

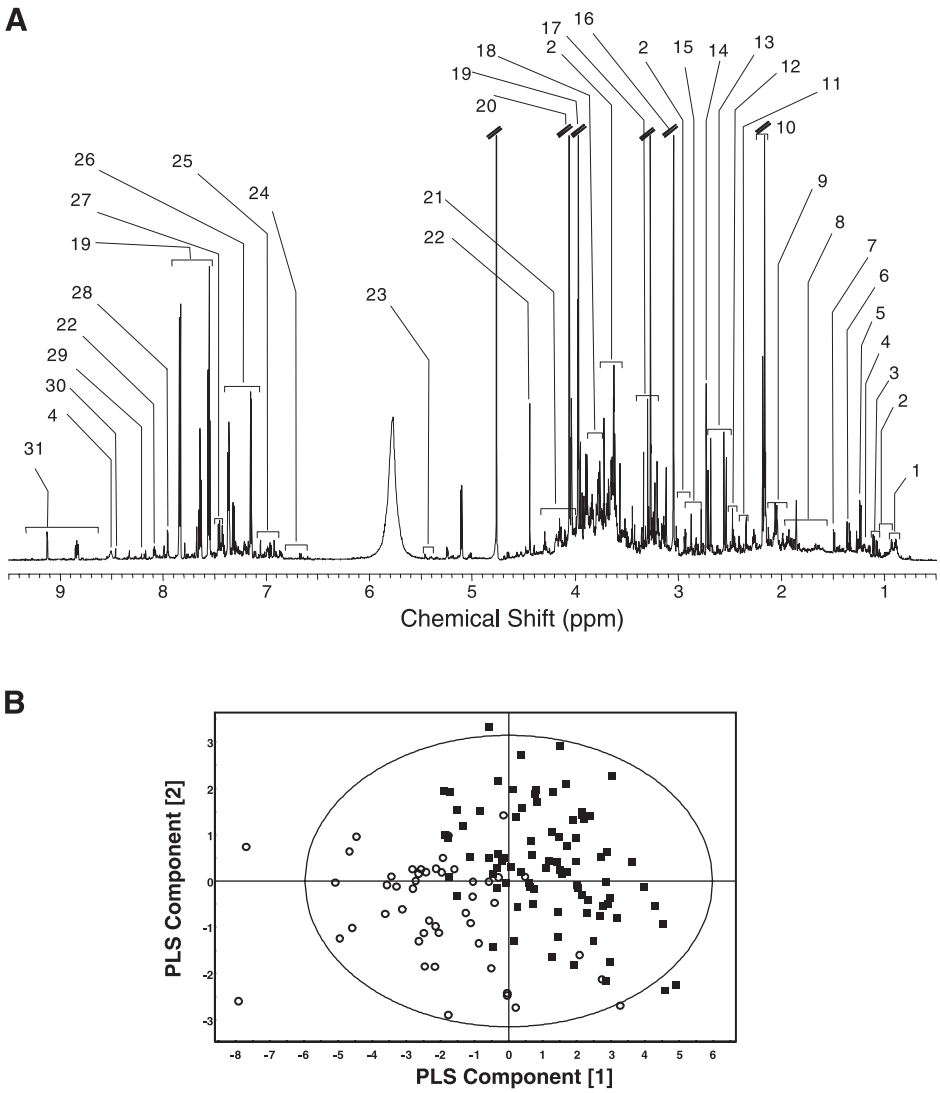

Fig. 3. Metabolomic analysis of human urine. *A*: high-resolution 700-MHz ^{1}H-NMR spectrum of an aqueous urine sample from a healthy control volunteer with the relevant resonance assignments shown. Each resonance corresponds to a chemical moiety within a particular metabolite with the intensity proportional to the concentration of that metabolite. *1*, α-hydroxybutyrate/valerate; *2*, amino acids; *3*, valerate; *4*, unassigned; *5*, β-hydroxybutyrate; *6*, lactate; *7*, alanine; *8*, amino acids/ornithine; *9*, *N*-acetyl groups/aspartate/glutamate; *10*, methionine; *11*, oxalacetate/pyruvate; *12*, β-hydroxybutyrate/glutamine/glutamate; *13*, citrate; *14*, DMA; *15*, TMA/DMG; *16*, creatine/creatinine; *17*, taurine; *18*, PAG; *19*, hippurate; *20*, creatine/creatinine; *22*, uridine bases; *22*, NMN acid; *23*, allantoin; *24*, unassigned pyrimidine; *25*, 3-hydroxypropionic acid/tyrosine; *26*, meta-hydroxyphenyl-propionic acid (mHPPA) sulfate/indoxyl sulfate; *27*, PAG; *28*, *N*-methyl-2-pyridone-5-carboxamide (2PY); *29*, NMN amide; *30*, formate; *31*, NMN amide/NMN acid. *B*: PLS-DA score plot of the healthy subjects (■) compared with the type 2 diabetes mellitus (T2DM) patients (○).

and morphology (dilation with proteinaceous casts, loss of functional microvilli on epithelium) (6). Hypertension and acquired dopamine D1 receptor dysfunction have also been reported in Zucker rats (3). Reduced GFR and substantial glomerular pathology, including mesangial matrix expansion and albuminuria, were reported for the *db/db* mouse along with nephropathy (28) and a decline in creatinine clearance after 5 mo of age (1).

Thus the observed changes in urinary metabolite concentration in the rodent models suggest early stage renal effects. However, the selection criteria employed for human subjects ensure no significant renal dysfunction for this data set. Because the changes in urinary metabolite concentration in the rodent models mirror those in the human samples, it is unlikely that the changes observed in the mouse and rat urine result solely from renal dysfunction, and most likely only represent early impairment of renal dysfunction.

Proteinuria in db/db mouse. High levels of protein were present in some of the mouse samples, especially in the *db/db* samples. The time scale of this effect and its presence also in C57/B16 wildtype mice suggested that it was independent of altered glomerular function (see above). Because of the broad resonances associated with these proteins, it was not possible to either identify individual proteins or reliably quantify these resonances, although their contribution was higher in male diabetic mice compared with all the other groups.

TCA cycle and fatty acid β-oxidation intermediates. Increases in relative concentrations of the TCA cycle intermediates citrate, malate, fumarate, and *cis*-aconitate were observed in the *fa/fa* rats and *db/db* mice but not in humans. Urinary excretion of these metabolites has previously been correlated inversely and nonspecifically with renal and hepatic toxicity as well as general stress (e.g., calorie restriction or neurological disease) (4, 12, 20, 24). The *db/db* mice and *fa/fa* rats have glycosuria, and it is possible that the correlated increases in urinary concentrations of TCA cycle intermediates reflect either systemic stress produced by hyperglycemia or local effects on kidney tubular transport.

Conversely, in human T2DM patients, relative decreases in malate, fumarate, and succinate were observed. Most human subjects exhibited more modest hyperglycemia compared with the two rodent models, suggesting that they had good dietary control of diabetes and consequently reduced manifestations of

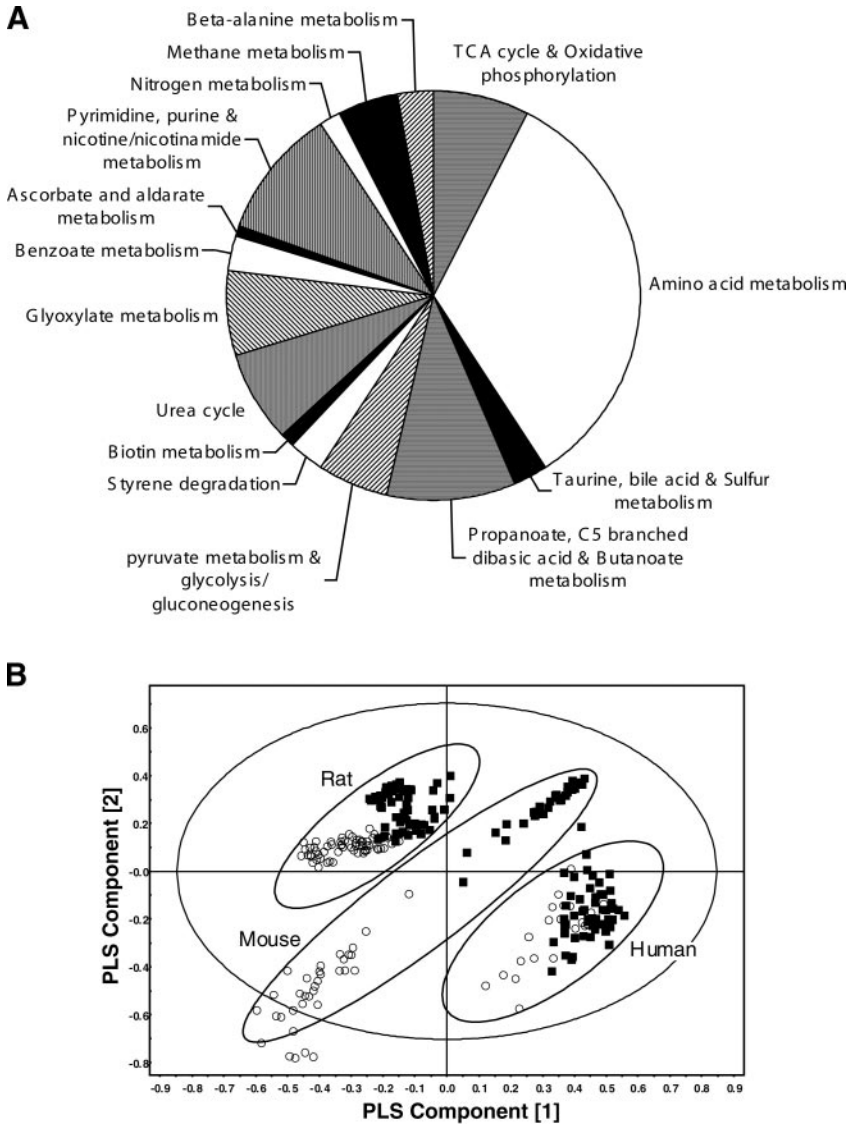

Fig. 4. Combined analysis of the metabolomic dataset. *A*: summary of the metabolic perturbations detected in urine from the two animal models of type 2 diabetes and sufferers of the disease. The Kyoto Encyclopedia of Genee and Genmes (KEGG) database was searched for each metabolite detected as perturbed and each KEGG pathway scored according to the number of metabolites listed within that pathway. For simplicity, some related pathways have been combined to form a single group. *B*: PLS-DA scores plot for male diabetic and control samples for human, rat, and mouse (R^2 = 0.57%, Q^2 = 0.59%, 3 components). Clear species separation exists between human, mouse, and rat samples, although all three models demonstrate separation between control samples (■) and disease samples (○) along the same principal component (PC).

accompanying pathologies (hepatic gluconeogenesis, insulin insensitivity, and renal dysfunction).

In diabetic patients and the animal models of T2DM, ketone bodies and fatty acids were increased in concentration. In humans this included acetate, acetoacetate, *n*-butyrate, α-hydroxy-*n*-butyrate, and β-hydroxybutyrate, which result from increased β-oxidation (45). In *fa/fa* rats, there was increased urinary excretion of short/medium chain fatty acids, although acetate and acetoacetate were decreased. These effects indicate an impairment of adipose tissue storage of circulating fatty acids and inhibition of hepatic fatty acid esterification. Both arise from insulin insensitivity causing increased concentrations of nonesterified fatty acids in blood plasma (34) and ultimately increased partial β-oxidation of fatty acids in the liver and skeletal muscle producing short chain fatty acids and ketone bodies (16).

Amino acid metabolism. End-stage diabetes, especially type 1 diabetes, is typified by the conversion of protein into glucose via gluconeogenesis. In the *db/db* mouse, observed metabolic perturbations indicated decreased excretion of amino acids, possibly reflecting increased clearance of these metabolites by the liver for gluconeogenesis, exacerbating the control of hyperglycemia. While there were comparable decreases in leucine, isoleucine, valine, histidine, and tryptophan in diabetic patients, an increase in glutamine and ornithine excretion was detected, suggesting that the perturbations in amino acid metabolism were more complex than simply an increase in gluconeogenesis in the liver.

Because of resonance overlap with glucose, the changes in taurine excretion could only be inferred using visual inspection. However, with this approach, taurine was observed to be increased in both animal models and the human patients. Although urinary taurine concentration is primarily regulated by renal reabsorption, the reabsorption is in turn regulated by taurine availability. Thus the increased excretion of taurine may arise from altered renal reabsorption of taurine as a result of reduced GFR or possibly as a general stress response, particularly following damage to the liver (22). Hypertaurinuria has also been detected following xenobiotic-induced perturbations in hepatic protein synthesis and other hepatotoxicities (4, 42).

Nucleotide metabolism. In T2DM patients, a relative increase in NMN amide and 2PY with a decrease in NMN acid was observed with similar changes in the *db/db* mouse and *fa/fa* rat. NMN amide is involved in the tryptophan-NAD^+ pathway, which supplies pyridine nucleotides to the liver (44). NMN amide can be further metabolized to 2PY and 4PY. 2PY formation appears to predominate over 4PY in humans and vice versa in rodents. NMN amide and 4PY have been suggested as urinary and plasma biomarkers of peroxisome proliferation in rats (10, 36). Plasma 2PY also increases with age in humans and in those with renal problems, possibly as a consequence of decreased renal excretion (38). Allantoin, a degradation product of nucleotide metabolism, is decreased in all three species, suggestive of a profound change in nucleotide metabolism during T2DM. It is interesting to note the commonalities between the perturbations reported in nucleotide metabolism in peroxisome proliferation and those observed here for T2DM. Peroxisome proliferation can only be confirmed by electron microscopy of the liver tissue, which was not carried out on either of the rodent models and of course is precluded from the routine analysis of human patients.

Analysis of the correlation of urinary nucleotide concentrations with clinical measures of T2DM revealed that changes in nucleotide metabolism reflect the direct metabolic consequences of the disease and are not the result of secondary complications (see Supplemental Materials for a detailed discussion of the correlation analysis). This included a negative correlation between the ratio of 2PY/NMN acid with HDL ($R^2 = 0.38 \pm 0.12$ for men and $R^2 = 0.49 \pm 0.08$ for women), although this correlation showed a distinct gender bias. Interestingly, the correlation between adiponectin and 2PY showed a positive correlation in males but a negative correlation in females, underlying the distinct interaction between gender and disease for T2DM.

Age progression and gender effects on metabolism in diabetes. By use of PLS to model metabolic changes with aging, the mouse and rat diabetic animals demonstrated different aging trends compared with control animals. The older diabetic animals were characterized by increased β-hydroxybutyrate and acetone and decreased citrate, 2-oxoglutarate, and fumarate relative to younger diabetic animals, with these trends not detected in the control group, suggesting that, in the older animals, increased insulin insensitivity has led to mitochondrial metabolism of acetyl-CoA increasingly via the 3-hydroxy-3-methyl-glutaryl-CoA cycle compared with the TCA cycle. Older *db/db* mice were characterized by decreased NMN amide, hippurate, mHPPA, and indoxyl sulfate relative to younger mice. Other effects observed include diurnal metabolite changes, consistent with the hormonal and sleep/wake cycles in Zucker rats.

A combined model of T2DM. A single PLS-DA model of T2DM was built using the NMR data from the mouse and rat models and from the human T2DM patients (Fig. 4*B*). In the scores plot, there is distinct species separation between the mouse, rat, and human samples with the separation being primarily due to relative changes in concentration of 2-oxoglutarate/creatine, citrate, DMA, and creatinine, with rats exhibiting a relative decrease in 2-oxoglutarate/creatine, citrate, and DMA and humans an increase in creatinine. However, all three groups demonstrate clear disease/wild-type separation along a common axis, indicating a similar disease process in each of the three species, with the differences among species being perpendicular to the differences associated with disease in our analysis.

The pathways highlighted as being affected by T2DM according to our metabolomic analysis (Fig. 4*A*) tally closely with gene transcript changes detected in the liver of *db/db* mice during treatment with metformin, a widely used hypoglycemic agent used in the treatment of T2DM acting to reduce hepatic gluconeogenesis and increase peripheral sensitivity to insulin (23). Heishi et al. (23) report changes in glycolysis/gluconeogenesis, TCA cycle, pyruvate metabolism, bile acid biosynthesis, lysine degradation, arginine and proline metabolism, and tryptophan metabolism; all of these pathways were similarly perturbed by T2DM in this study. Along with the expected changes in hepatic glycolysis/gluconeogenesis, TCA cycle, and pyruvate and fatty acid metabolism, significant changes in hepatic amino acid metabolism were observed including tryptophan metabolism. Tryptophan is a precursor for nicotinate from which NMN amide, 2PY, and 4PY are produced. A summary of the metabolite changes observed in all three models of T2DM is given in Table 1.

In conclusion, our metabolomic analyses of urine from two rodent models of diabetes and human patients with T2DM have highlighted several metabolic processes that are perturbed in all three species. In addition to the expected glycosuria and changes in energy metabolism (gluconeogenesis, fatty acid oxidation), all three species demonstrated profound changes in nucleotide metabolism. The effects in NMN amide and 2PY metabolism may provide novel biomarkers for following the progression of T2DM.

Table 1. *Summary of metabolic changes observed in rodent models and human subjects*

Metabolite	Change in T2DM
Methylamine metabolism, TMA, DMA, DMG, betaine, TMAO	↑
Creatine, creatinine	↓
TCA cycle	
Citrate	↑
Malate, fumarate, succinate	↑ (r) ↓ (h)
2-Oxoglutarate	?(r) ↓ (h)
Fatty acid metabolism	
Acetate, acetoacetate	↓ (r) ↑ (h)
n-Butyrate, α-hydroxy-*n*-butyrate, β-hydroxybutyrate	↑
Amino acid metabolism	
Alanine	↓ (r), ↑ (h)
Leucine, isoleucine, histidine, tryptophan	↓
Glutamine	↑
Ornithine	↓ (r) ↑ (h)
Taurine	↑
Nucleotide metabolism	
NMN amide	↑
NMN acid	↓
2PY	↑
Allantoin	↓

Changes listed are for both human and rodent models unless marked "(h)" or "(r)", respectively. "?" Overlapped resonance making the direction of change ambiguous. T2DM, type 2 diabetes mellitus; TMA, trimethylamine; DMA, dimethylamine; DMG, *N,N*-dimethylglycine; TMAO, trimethylamine-*N*-oxide; NMN amide, *N*-methylnicotinamide; NMN acid, *N*-methylnicotinate; 2PY, *N*-methyl-2-pyridone-5-carboxamide.

GRANTS

This work was supported by grants from GlaxoSmithKline, The Royal Society (a University Research Fellowship to J. L. Griffin), and the Wellcome Trust. R. D. Cox is supported by European Union (EU) FP5 Grant EURAGEDIC QLG2-CT-2001-01669.

REFERENCES

1. **Allen TJ, Cooper ME, Lan HY.** Use of genetic mouse models in the study of diabetic nephropathy. *Curr Diab Rep* 4: 435–440, 2004.
2. **Asatoor AM, Simenhoff ML.** The origin of urinary dimethylamine. *Biochim Biophys Acta* 111: 384–392, 1965.
3. **Banday AA, Hussain T, Lokhandwala MF.** Renal dopamine D(1) receptor dysfunction is acquired and not inherited in obese Zucker rats. *Am J Physiol Renal Physiol* 287: F109–F116, 2004.
4. **Beckwith-Hall BM, Nicholson JK, Nicholls AW, Foxall PJ, Lindon JC, Connor SC, Abdi M, Connelly J, Holmes E.** Nuclear magnetic resonance spectroscopic and principal components analysis investigations into biochemical effects of three model hepatotoxins. *Chem Res Toxicol* 11: 260–272, 1998.
5. **Briggs JP, Levitt MF, Abramson RG.** Renal excretion of allantoin in rats: a micropuncture and clearance study. *Am J Physiol Renal Fluid Electrolyte Physiol* 233: F373–F381, 1977.
6. **Buckingham RE, Al-Barazanji KA, Toseland CD, Slaughter M, Connor SC, West A, Bond B, Turner NC, Clapham JC.** Peroxisome proliferator-activated receptor-gamma agonist, rosiglitazone, protects against nephropathy and pancreatic islet abnormalities in Zucker fatty rats. *Diabetes* 47: 1326–1334, 1998.
7. **Christiansen JS, Gammelgaard J, Frandsen M, Parving HH.** Increased kidney size, glomerular filtration rate and renal plasma flow in short-term insulin-dependent diabetics. *Diabetologia* 20: 451–456, 1981.
8. **Chung YL, Rider LG, Bell JD, Summers RM, Zemel LS, Rennebohm RM, Passo MH, Hicks J, Miller FW, Scott DL.** Muscle metabolites, detected in urine by proton spectroscopy, correlate with disease damage in juvenile idiopathic inflammatory myopathies. *Arthritis Rheum* 53: 565–570, 2005.
9. **Clark JB, Palmer CJ, Shaw WN.** The diabetic Zucker fatty rat. *Proc Soc Exp Biol Med* 173: 68–75, 1983.
10. **Connor SC, Hodson MP, Ringeissen S, Sweatman BC, McGill PJ, Waterfield CJ, Haselden JN.** Development of a multivariate statistical model to predict peroxisome proliferation in the rat, based on urinary 1H-NMR spectral patterns. *Biomarkers* 9: 364–385, 2004.
11. **Connor SC, Hughes MG, Moore G, Lister CA, Smith SA.** Antidiabetic efficacy of BRL 49653, a potent orally active insulin sensitizing agent, assessed in the C57BL/KsJ db/db diabetic mouse by non-invasive 1H NMR studies of urine. *J Pharm Pharmacol* 49: 336–344, 1997.
12. **Connor SC, Wu W, Sweatman BC, Manini J, Haselden JN, Crowther DJ, Waterfield CJ.** Effects of feeding and body weight loss on the 1H-NMR-based urine metabolic profiles of male Wistar Han rats: implications for biomarker discovery. *Biomarkers* 9: 156–179, 2004.
13. **Coomans D, Broeckaert I, Derde MP, Tassin A, Massart DL, Wold S.** Use of a microcomputer for the definition of multivariate confidence regions in medical diagnosis based on clinical laboratory profiles. *Comput Biomed Res* 17: 1–14, 1984.
14. **Eriksson I, Johansson E, Kettaneh-Wold N, Wold S.** *Multi- and Megavariate Data Analysis. Principles and Applications*. Umea, Sweden: Umetrics Acedemy, 2001.
15. **Fan TWM.** Metabolite profiline by one- and two-dimensional NMR analysis of complex mixtures. *Prog Nuclear Mag Res Spectros* 28: 161–219, 1996.
16. **Frayn K.** *Metabolic Regulation: A Human Perspective*. Oxford, UK: Blackwell Science, 2003.
17. **Garcia-Perez A, Burg MB.** Role of organic osmolytes in adaptation of renal cells to high osmolality. *J Membr Biol* 119: 1–13, 1991.
18. **Gavaghan CL, Holmes E, Lenz E, Wilson ID, Nicholson JK.** An NMR-based metabonomic approach to investigate the biochemical consequences of genetic strain differences: application to the C57BL10J and Alpk:ApfCD mouse. *FEBS Lett* 484: 169–174, 2000.
19. **Greger R, Lang F, Deetjen P.** Handling of allantoin by the rat kidney. Clearance and micropuncture data. *Pflügers Arch* 357: 201–207, 1975.
20. **Griffin JL.** Metabolic profiles to define the genome: can we hear the phenotypes? *Philos Trans R Soc Lond B Biol Sci* 359: 857–871, 2004.
21. **Gullans SR, Heilig CW, Stromski ME, Blumenfeld JD.** Methylamines and polyols in kidney, urinary bladder, urine, liver, brain, and plasma. An analysis using 1H nuclear magnetic resonance spectroscopy. *Renal Physiol Biochem* 12: 191–201, 1989.
22. **Han X, Patters AB, Jones DP, Zelikovic I, Chesney RW.** The taurine transporter: mechanisms of regulation. *Acta Physiol (Oxf)* 187: 61–73, 2006.
23. **Heishi M, Ichihara J, Teramoto R, Itakura Y, Hayashi K, Ishikawa H, Gomi H, Sakai J, Kanaoka M, Taiji M, Kimura T.** Global gene expression analysis in liver of obese diabetic db/db mice treated with metformin. *Diabetologia* 49: 1647–1655, 2006.
24. **Holmes E, Nicholls AW, Lindon JC, Ramos S, Spraul M, Neidig P, Connor SC, Connelly J, Damment SJ, Haselden J, Nicholson JK.** Development of a model for classification of toxin-induced lesions using 1H NMR spectroscopy of urine combined with pattern recognition. *NMR Biomed* 11: 235–244, 1998.
25. **Hough TA, Nolan PM, Tsipouri V, Toye AA, Gray IC, Goldsworthy M, Moir L, Cox RD, Clements S, Glenister PH, Wood J, Selley RL, Strivens MA, Vizor L, McCormack SL, Peters J, Fisher EM, Spurr N, Rastan S, Martin JE, Brown SD, Hunter AJ.** Novel phenotypes identified by plasma biochemical screening in the mouse. *Mamm Genome* 13: 595–602, 2002.
26. **Ismail AA, Gill GV.** The epidemiology of Type 2 diabetes and its current measurement. *Baillieres Best Pract Res Clin Endocrinol Metab* 13: 197–220, 1999.
27. **Korner A, Eklof AC, Celsi G, Aperia A.** Increased renal metabolism in diabetes. Mechanism and functional implications. *Diabetes* 43: 629–633, 1994.
28. **Lee SM, Graham A.** Early immunopathologic events in experimental diabetic nephropathy: a study in db/db mice. *Exp Mol Pathol* 33: 323–332, 1980.
29. **Leon CA, Raij L.** Interaction of haemodynamic and metabolic pathways in the genesis of diabetic nephropathy. *J Hypertens* 23: 1931–1937, 2005.
30. **Lindon JC, Nicholson JK, Everett JR.** NMR spectroscopy of biofluids. *Annu Rep NMR Spectros* 38: 1–88, 1999.
31. **Mantzoros CS.** The role of leptin in human obesity and disease: a review of current evidence. *Ann Intern Med* 130: 671–680, 1999.
32. **Prasad K.** Secoisolariciresinol diglucoside from flaxseed delays the development of type 2 diabetes in Zucker rat. *J Lab Clin Med* 138: 32–39, 2001.
33. **Pugliese G, Tilton RG, Williamson JR.** Glucose-induced metabolic imbalances in the pathogenesis of diabetic vascular disease. *Diabetes Metab Rev* 7: 35–59, 1991.
34. **Reaven GM, Chen YD.** Role of abnormal free fatty acid metabolism in the development of non-insulin-dependent diabetes mellitus. *Am J Med* 85: 106–112, 1988.
35. **Reed MJ, Scribner KA.** In-vivo and in-vitro models of type 2 diabetes in pharmaceutical drug discovery. *Diabetes Obes Metab* 1: 75–86, 1999.
36. **Ringeissen S, Connor SC, Brown HR, Sweatman BC, Hodson MP, Kenny SP, Haworth RI, McGill P, Price MA, Aylott MC, Nunez DJ, Haselden JN, Waterfield CJ.** Potential urinary and plasma biomarkers of peroxisome proliferation in the rat: identification of *N*-methylnicotinamide and *N*-methyl-4-pyridone-3-carboxamide by 1H nuclear magnetic resonance and high performance liquid chromatography. *Biomarkers* 8: 240–271, 2003.
37. **Roesler WJ, Pugazhenthi S, Khandelwal RL.** Hepatic glycogen metabolism in the db/db mouse. *Mol Cell Biochem* 92: 99–106, 1990.
38. **Slominska EM, Rutkowski P, Smolenski RT, Szutowicz A, Rutkowski B, Swierczynski J.** The age-related increase in *N*-methyl-2-pyridone-5-carboxamide (NAD catabolite) in human plasma. *Mol Cell Biochem* 267: 25–30, 2004.
39. **Stella C, Beckwith-Hall B, Cloarec O, Holmes E, Lindon JC, Powell J, van der Ouderaa F, Bingham S, Cross AJ, Nicholson JK.** Susceptibility of human metabolic phenotypes to dietary modulation. *J Proteome Res* 5: 2780–2788, 2006.
40. **Tasaka Y, Yanagisawa K, Iwamoto Y.** Human plasma leptin in obese subjects and diabetics. *Endocr J* 44: 671–676, 1997.
41. **Turner NC, Morgan PJ, Haynes AC, Vidgeon-Hart M, Toseland N, Clapham JC.** Elevated renal endothelin-I clearance and mRNA levels associated with albuminuria and nephropathy in non-insulin-dependent

diabetes mellitus: studies in obese fa/fa Zucker rats. *Clin Sci (Lond)* 93: 565–571, 1997.
42. **Waterfield CJ, Asker DS, Patel S, Timbrell JA.** Is there a correlation between taurine levels and xenobiotic-induced perturbations in protein synthesis?: a study with tetracycline in rats. *Amino Acids* 15: 161–177, 1998.
43. **White BD, Martin RJ.** Evidence for a central mechanism of obesity in the Zucker rat: role of neuropeptide Y and leptin. *Proc Soc Exp Biol Med* 214: 222–232, 1997.
44. **Wolf H.** The effect of hormones and vitamin B6 on urinary excretion of metabolites of the kynurenine pathway. *Scand J Clin Lab Invest* 136: 1–186, 1974.
45. **Yu WM, Kuhara T, Inoue Y, Matsumoto I, Iwasaki R, Morimoto S.** Increased urinary excretion of beta-hydroxyisovaleric acid in ketotic and non-ketotic type II diabetes mellitus. *Clin Chim Acta* 188: 161–168, 1990.
46. **Zimmet P, Alberti KG, Shaw J.** Global and societal implications of the diabetes epidemic. *Nature* 414: 782–787, 2001.
47. **Zucker LM, Antoniades HN.** Insulin and obesity in the Zucker genetically obese rat "fatty". *Endocrinology* 90: 1320–1330, 1972.